International Journal of Impact Engineering 60 (2013) 120–132

Contents lists available at SciVerse ScienceDirect

International Journal of Impact Engineering

journal homepage: www.elsevier.com/locate/ijimpeng

Drop weight impact behaviour of sandwich panels with metallic micro lattice cores

R.A.W. Mines*, S. Tsopanos, Y. Shen, R. Hasan, S.T. McKown

School of Engineering, University of Liverpool, The Quadrangle, Liverpool L69 3GH, UK

ARTICLE INFO

Article history:
Received 23 October 2012
Received in revised form
8 April 2013
Accepted 19 April 2013
Available online 29 April 2013

Keywords:
Drop weight
Sandwich panel
Micro lattice structures
Titanium alloy
Stainless steel

ABSTRACT

The paper addresses the low velocity, drop weight behaviour of small (100 mm by 100 mm) sandwich panels with CFRP skins. The main point of interest is the core material, and the focus of the paper is in the use of body centred cubic (BCC) micro lattice cores made from Ti 6Al 4V titanium alloy and 316L stainless steel manufactured using selective laser melting. The mechanical behaviour of the micro lattice core is compared to that of conventional aluminium honeycomb. The paper discusses the manufacture and characterisation of the core materials, the measurement of core properties from strut tensile tests, block compression tests and the drop weight impact performance of the panels. Impact performance is expressed in terms of panel penetration. It is shown that the current Ti 6Al 4V BCC micro lattice cores are competitive with aluminium honeycomb, but that there is scope for improvement in Ti 6Al 4V micro strut mechanical properties. The SLM manufacturing process gives lattice structures with open cell architecture, which is an advantage for aerospace applications, and the SLM process can be used to realise a variety of cell lattice geometries.

1. Introduction

Twin skinned, sandwich, structures are of interest for application for aerospace structures found in fuselage, wing and other components. Such structures have advantages over monolithic shells, such as improved specific bending stiffness and strength, and multi function potential, e.g. acoustic and thermal properties [1].

A feature of twin skinned construction is the cellular core. Conventionally in aerospace applications, the most widely used architecture is that of honeycomb, in either aluminium or aramid. However, such materials have the disadvantage of closed cells, when used with skins, which give rise to moisture and gas retention [2]. Recently, folded textile paper cores have been developed which have optimised mechanical properties but an open cell architecture [2]. Another class of open cell material is the metallic lattice structure [3]. This class of structure has been extensively studied theoretically, and although linear properties are well understood, further research is needed on strength and toughness issues [4]. Metallic lattice structures can be manufactured a number of ways, including using textile technology [3] and forming and brazing [5].

The focus for this paper is the study and use of a new, innovative, micro lattice core material manufactured using selective laser melting [SLM] [6,7]. In this process, metallic powder is selectively melted to form spatial micro lattice structures. Previous papers on micro lattice structures have discussed the manufacturing process for stainless steel micro lattices [8], some testing of micro lattice blocks and beams [9] and some theoretical parametric studies [10]. A feature of the SLM manufacturing process is the ability to realise lattice structures with 50 μm features, which means that the lattice structures can be tailored with the application in mind. Once the manufacturing process is refined, this shifts emphasis to detailed study and optimisation of cellular materials, which includes structural engineering at the small scale. Ushijima et al. [10] developed parametric compressive models for the body centred cubic micro lattice geometry in the form of blocks, and showed the complexity of parametric modelling. Labeas and Sunaric also analysed theoretically micro lattice blocks [11]. These ideas need to be developed further to include multiple collapse mechanisms, so as to fully exploit the manufacturing process.

It should be noted that there are other manufacturing processes for micro lattice structures. For example, micro lattice structures have been realised in thiol-ene polymer using ultra violet light [12]. Strut diameters of the order of 200 μm and cell sizes of the order of

* Corresponding author. Tel.: +44 151 794 4819; fax: +44 151 794 4848.
E-mail addresses: r.mines@liv.ac.uk, R.Mines@liverpool.ac.uk (R.A.W. Mines).

0734-743X
http://dx.doi.org/10.1016/j.ijimpeng.2013.04.007

Nomenclature

BCC	Body Centred Cubic
BCC, Z	Body Centred Cubic, with vertical (Z) struts
F2, BCC	Body Centred Cubic, with two diagonal face struts
SLM	Selective Laser Melting
SS316L	Stainless Steel 316L
Ti6 4	Titanium Alloy Ti 6Al 4V
E	Young's Modulus strut (GPa)
E_B	Compression Block Stiffness (GPa)
E_{SLM}	Young's Modulus of strut – SLM (GPa)
E_{TB}	Young's Modulus of strut – Text book (GPa)
HIP	Hot Isostatic Processing
L	Length of BCC Cell (m)
N	Number of BCC Cells
V	Block Material Volume (m^3)
d	Strut diameter (μm)
m_b	Mass of BCC block (kg)
ε_{fB}	Block compression failure strain
ε_f	Strut tensile failure strain
ε_{fSLM}	Strut tensile failure strain – SLM
ε_{fTB}	Strut failure strain – Text book
ρ_p	Density of parent material (kgm^{-3})
ρ^*	Density of BCC block (kgm^{-3})
ρ_R	Block relative density $= \rho^*/\rho_p$
σ_{2B}	Crush Stress BCC Block at 2% strain (MPa)
$\sigma_{0.2}$	0.2% Proof Stress Strut (MPa)
$\sigma_{0.2SLM}$	0.2% Proof Stress Strut from SLM (MPa)
$\sigma_{0.2TB}$	0.2% Proof Stress Strut from Text book (MPa)
σ_{ultB}	Ultimate Compression Strength Block (MPa)
σ_{uts}	Ultimate Tensile Strength Strut (MPa)
σ_{utsSLM}	Ultimate Tensile Strength Strut from SLM (MPa)
σ_{utsTB}	Ultimate Tensile Strength Strut from Text book (MPa)
σ_0	Flow stress of parent material (MPa)
σ_{pl}	Block collapse stress (MPa)

1 mm have been obtained. This technique has been extended to the manufacture of hollow nickel ultra light micro lattice structures using electro deposition, with a density of 1 kgm^{-3}, a micro strut diameter of 200 μm and a strut wall thickness of 100 nm [13]. Ti 6 4 micro lattice structures have been realised using Electron Beam Melting. Parthasarathy et al. [14] realised rectangular micro structures with a cell size of 2 mm and a strut diameter of 800 μm. Cansizoglu et al. [15] realised a hexagonal/rectangular hybrid micro lattice structure with a cell size of 5 mm and a strut diameter of 500 μm. Electron beam melting is faster and more economic compared to selective laser melting, but the surface quality of components is not as good [16]. A common theme in these papers is ensuring good mechanical properties for parent materials and ensuring good quality lattice construction. The definition of the process-material-property relation has been identified as being critical for the full exploitation of additive manufacturing technology [16]. These issues will be addressed in this paper.

It should be noted that a major issue with additive layer manufacture, e.g. selective laser melting (SLM), is the potential to create actual metallic engineering components [16]. This requires not only full definition of the performance of the component (the subject of this paper), but also ensuring that the cost and environmental performance of the manufacturing process are competitive, or better than, state of the art structural solutions. The selective laser melting process is still being improved, and Kellens et al. [17] identify the need to improve machine costs, energy and gas consumption, production time, and amount of waste (contaminated powder). Aerospace companies are investigating the potential of selective laser melting, and other additive layer manufacturing processes, for the manufacture of small numbers of high value structural components. Work on qualifying SLM on civil aircraft has begun with low risk parts for secondary structures, e.g. stainless steel fan cowl brackets and hinges [18]. This qualification work concerns solid SLM components, and the thin sectioned micro lattice struts discussed here are currently at a lower level of technology readiness.

One of the major performance issues of aerospace twin skinned construction is their foreign object impact performance [19]. This can be a result of dropped tools, hail, runway debris, and bird strike. Impact can give rise to sub critical damage, or partial and full penetration. This paper addresses the drop weight impact scenario [20]. Impact behaviour is dependent on the skin and the core, and in this paper, the focus will primarily be on cores, and both lattice and honeycomb architectures will be considered.

The impact dynamics of cellular architectures have been studied extensively in the literature. Smith et al. [21] studied the blast performance of stainless steel micro lattices, similar to those discussed here. They identified material strain rate as being an important strengthening mechanism. Lee et al. [22] studied the impact response of a single cell thickness pyramidal core, and Lee et al. [23] studied a multiple layer lattice core. They identified the effects of micro inertia and strain rate, and showed the importance of assessing structural imperfections. Evans et al. [24] analysed the impact performance of hollow nickel lattices, similar but on a larger scale to those discussed in [13]. They identified local and global buckling effects on energy absorption. In the case of honeycomb, Fang and Zhao [25] tested specimens in combined compression and shear, and they showed a doubling of crush stress. Mahmoudabadi and Sadighi [26] highlighted the change in collapse mode for honeycomb blocks under static and impact compression. Hence, the architecture and parent material of the cellular core will influence the impact effects of structural micro inertia and material strain rate.

This paper extends previous discussions on stainless steel 316L micro lattices to Titanium Alloy Ti 6 4 [27] micro lattice structures, and to drop weight impact performance of small sandwich panels. Panel performances are compared to panels with conventional aluminium honeycomb cores. The bases for performance comparisons are for a single strut, a block of material, and a complete, small, panel. The criteria for impact performance of panels are penetrator penetration and extent of damage [28].

2. The micro lattice cores

In the SLM manufacturing process [8], a fibre optic laser selectively melts the powder (laser spot size = 90 μm), with layers of powder (depth = 50 μm) being added after each laser pass. The selective laser melting machine used here is an MCP Realiser II (MCP HEK Tooling Gmbh, Lubeck, Germany) commissioned in 2006 and with a 250 mm × 250 mm × 250 mm build volume [8]. The lattice geometry, whether block or strut, is defined in Manipulator software [29] and the geometric data is then converted into a machine form using Realizer software [30]. The laser is moved from point to point in 3D space, and laser parameters such as scanning strategy, exposure time and power are selected. To minimize strand diameter, the structures are built from single laser point exposures. This result in the strut diameter being

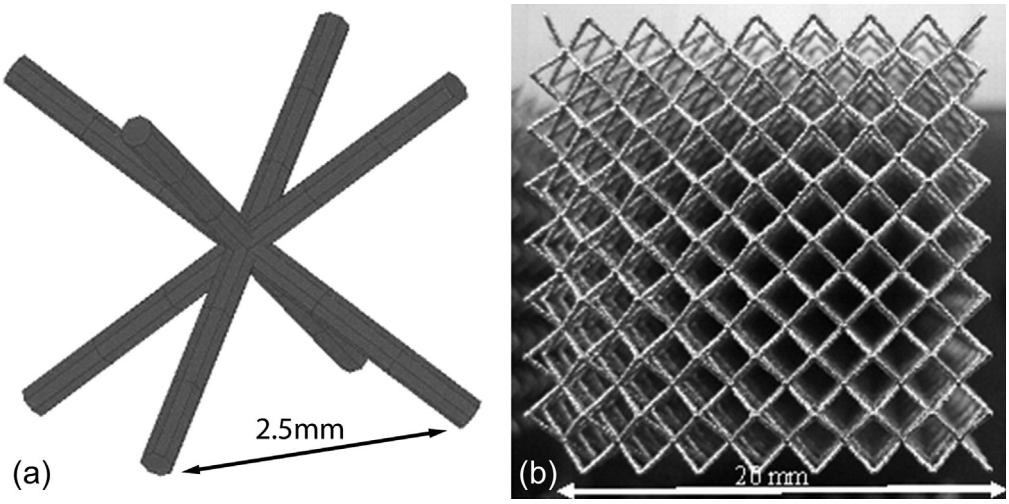

Fig. 1. BCC geometry: (a) Cell detail and (b) 20 mm × 20 mm × 20 mm block.

equal to the diameter of the laser melt pool produced by each exposure [31].

The micro lattice geometry realised is shown in Fig. 1. We call this body centred cubic (BCC) [7]. This is not optimal for stiffness and strength behaviour [7,32,33], but has the advantages of ease and reliability of manufacture [8], and of simplicity of response for multi axial deformation [9].

Important properties for cellular cores are specific stiffness and strength. Stainless steel 316L micro lattice structures are not competitive with aluminium honeycomb under compression [34], and so there is a need for more lightweight parent materials and Ti 6 4 is a widely used lightweight alloy, used especially in the aerospace industry [27]. However, Ti 6 4 is a much more complex material compared to SS316L and is more difficult to manufacture using the selective laser melting process.

The major manufacturing parameters in the selective laser melting process are laser exposure time and laser power [8]. It has been shown that, for the 316L stainless steel parent material, these parameters influence strut diameter and strut mechanical strength. For the stainless steel case, the laser power was selected as 140 W and the laser exposure time was selected as 500 μs [8]. The criteria for selection were acceptable mechanical properties with reasonable manufacturing times. Fig. 2(a) gives the tensile engineering stress strain data for a single micro strut built at 90° (vertical) – details of the procedure and repeatability issues are addressed in [8]. One of the major themes of this paper is the relation of these mechanical properties to text book/best data. Fig. 2(b) shows the quality of the strut and highlights dimensional accuracy and surface quality issues. In deriving the stress strain data for Fig. 2(a), the cross sectional area from a minimum diameter of 197 μm was taken from photos of sectioned micro struts, and a circular cross section was assumed.

3. Ti 6 4 micro strut and mechanical properties

Ti 6 4 is a widely used titanium alloy in the aerospace industry [27]. In the case of selective laser melting, the material is provided as a fine powder from TLS Technik [35]. Fig. 3 gives powder details and Table 1 gives the chemical composition. The fine (45 μm) powder was used. The alloy is complex and can be subject to a variety of post manufacture treatments.

In the case of Ti 6 4, given the complexity of its metallurgy, there is scope for much more variability in mechanical properties. However, the same manufacturing machine and conditions were used for Ti 6 4, as for SS316L [8], apart from laser power and exposure time. A systematic parametric variation for laser power (140–200 W) and for laser exposure time (500–1000 μs) was conducted, in which 20 mm^3 BCC blocks were manufactured, studied and compression tested. The main laser parameters selected for the Ti 6 4 micro lattice core were laser power = 200 W and laser exposure time of 1000 μs, as these gave the strongest structures although the material ductility was reduced. These parameters gave a typical micro strut diameter

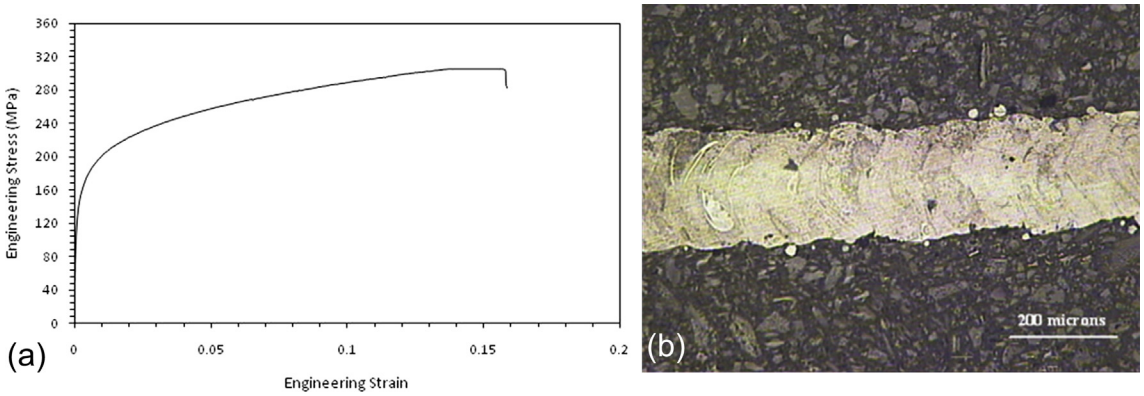

Fig. 2. Stainless steel 316L (a) Compliance corrected engineering stress strain data with clip gauge for strut built at 90° angle (vertical). Power = 140 W and Exposure Time = 500 μs, E = 140 GPa, yield stress = 144 MPa (b) detail of strut (200 W/1000 μs) showing quality of geometry and surface [8]. Strut diameter = 197 ± 17 μm.

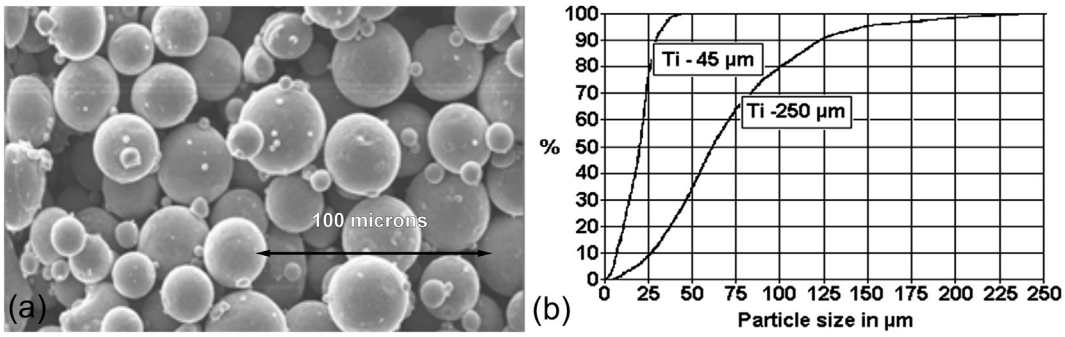

Fig. 3. (a) SEM image of 45 μm Ti 6 4 micro powder and (b) particle size distribution for fine (45 μm) and medium (250 μm) average [35].

of 372 μm. 180 W × 500 μs micro lattices were also selected for study, for comparison.

In order to determine the basic mechanical properties of titanium alloy (Ti 6 4) micro lattice structures, it is important to analyse single struts. Therefore, single struts were manufactured using the same parameters as those for micro lattice panel cores, which was at 200 W laser power and 1000 μs laser exposure time. The rest of the manufacturing conditions were assumed to be the same. Since the orientation of micro struts in the BCC architecture was at 35° angle from horizontal, the single struts were manufactured at 35° build angle, with maximum length limited to 43 mm. However, it should be noted that there might be some effect in properties if different build angle, such as 90° (vertical), is being used in producing the single struts. As reported by Shen [36], the titanium alloy struts built at an angle of 35° have a higher (14%) diameter than the struts built vertically.

The tensile tests were conducted on a small bench top servo-hydraulic testing machine (Instron (Norwood, USA) 3342 machine), with 500 N load-cell. Loading velocity of 0.1 mm/min was applied throughout the test, but without the application of extensometer for strain measurement. The strain was derived directly from the crosshead displacement and a compliance correction method as described in [37] and [38] was used. The issue here is the dependence of stiffness and strength on the gauge length of the micro strut specimen. A complex, but verified, procedure for wire testing was followed in which the compliance of the testing machine was assessed [37]. Limited by the manufactured specimen length, only five different gauge lengths L, were tested, which were 5 mm, 8 mm, 10 mm, 22 mm and 30 mm, with three repeat tests for each gauge length. Measurement of diameter and cross-sectional area for stress calculations was taken from a number of cross sectional photos, and an averaging methodology for assessing diameter variation was used. A diameter value of 372 ± 28 μm was used. Another major issue is strut circularity which has been addressed for stainless steel [8] and Ti 6 4 [38]. Hence, the accuracy of stress values is dependent on accuracy of micro strut geometry measurement.

Fig. 4(a) gives compliance corrected data for three Ti 6 4 strut tests. Repeatability is shown to be good apart from strain to failure, which is also generally low. Fig. 4(b) shows that the surface quality of the micro strut is not as good as that for SS316L (Fig. 2(b)). Hasan et al. [38] have conducted a sustained study of the quality of the microstructure of Ti 6 4 lattices. They have shown that due to the complexity of the formation of the micro lattice, during SLM, there is non-optimal material microstructure and associated mechanical properties.

Table 1
Chemical composition of Ti 6 4 powder[35].

Element	Al	V	Fe	Si	O	C	N	H
Ti 5 max.	5.5–6.5	3.4–4.5	0.25	n.a.	0.13	0.08	0.05	0.012
Ti 5 typical	5.9	3.9	0.19	n.a.	0.12	0.01	0.01	0.004

At this point, it is instructive to compare strut mechanical properties for material produced using selective laser melting with text book values. Table 2 summarises test data and compares values with those from published data [39–41]. It should be noted that the mechanical properties for Al 5056 are for the H38 temper, as mechanical property data for H39 temper (as used in the honeycombs studied here) has not been published in the open literature. H39 Tempered material has higher strength but reduced ductility over the H38 Temper. As far as SS316L is concerned, the elastic modulus is 67% of the text book value. The yield stress for SLM is about half that for text book values. This is most likely due to imperfection sensitivity for SLM structures. A similar state of affairs occurs for the ultimate tensile strength (UTS). A feature of SLM produced micro struts is their low strain to failure. Disagreement for Ti 6 4 is greater, again showing the complexity and sensitivity of this material system. In order to improve Ti 6 4 properties, a post manufacture treatment of Hot Isostatic Processing was considered (see below). Low values of material properties are attributed to micro strut surface quality, dimensional quality (including circularity), complexity of microstructure, and possible residual stresses. Stress calculations assume a circular cross section and a cylindrical shape. It has been shown that the struts depart from this idealisation as the angle of build tends to the horizontal plane [36]. Also, variation in surface quality will give rise to stress raisers, which will affect plasticity and rupture properties. These issues require further consideration of manufacture and materials, and these issues are discussed later.

4. Blocks 2.5 mm cell size (BCC) for Ti 6 4

The aims of these block tests were to study progressive collapse mechanisms for a simple loading case (compression), to provide a means of quantifying the effect of manufacturing parameters and heat treatment for Ti 6 4 and to allow detailed study of deformation at nodes in the BCC structure. As stated in the introduction, the micro lattice configuration studied here was body centred cubic (BCC) – see Fig. 1. Each block was 2.5 mm cell size and 20 mm cubed (8 cell cubed). The quality of individual struts has been discussed in the previous section.

An important structural detail that influences progressive collapse and foreign object panel impact behaviour is the BCC node. Fig. 5 gives details of this. The section is taken on the diagonal of the block and the build direction is from right to left. The black dots represent estimated laser focus points at different times, and the thin lines represent estimated globule boundaries. From the photo it can be seen that continuity of struts through the node is good and that there is little excess material. The quality of the node is dependent on the laser scanning strategy [8].

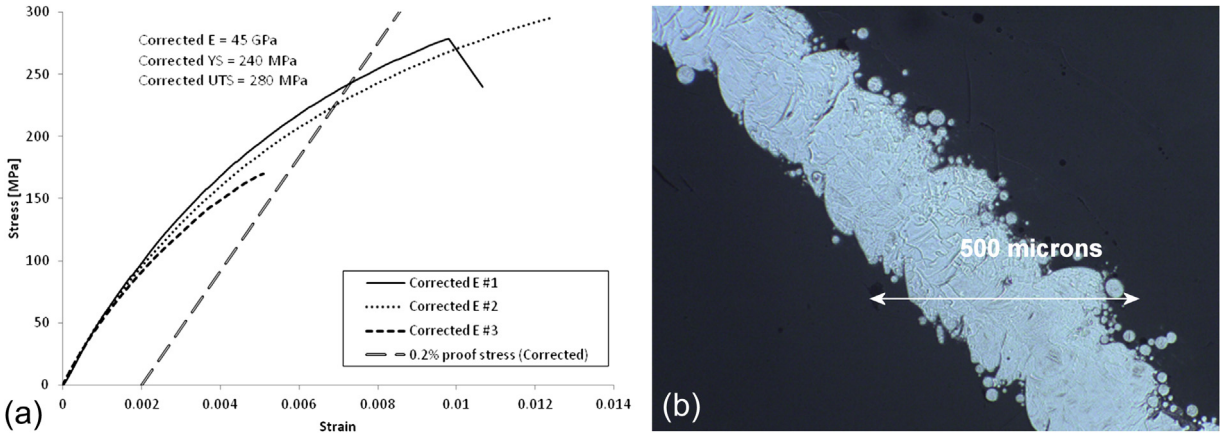

Fig. 4. Ti 6 4 micro strut test (a) 35° built micro strut engineering stress strain curves with compliance correction (as built 200 W laser power and 1000 μs laser exposure time) (b) Photo showing dimensional and surface quality of a micro strut (average diameter 372 ± 28 μm).

To summarise part of the manufacture process, in Fig. 5, the laser switches on at point A for $t = 1000$ μs. The laser then moves to point B and switches on for 1000 μs. The laser then moves on to other nodes and blocks. A number of blocks, e.g. 25, can be manufactured at any one time, or a mixture of specimens can be manufactured, e.g. micro struts and blocks [8]. The laser returns to point C in 30–60 s, and by this time the globule at A has solidified. The introduction of laser power at C melts the powder and partially melts globule A. Note, the build direction is at an incline of 45°. There is a complex thermo mechanical process here, and this is discussed in detail by Yadroitsev [6] and Rehme [7]. The thermo mechanical process will affect the quality of micro strut and node, and their geometry and properties.

The current state of affairs has been achieved through an empirical parametric approach [31], in a similar manner to Rehme [7]. There is further scope to rigorously study this thermo mechanical process in order to adjust micro strut and node manufacture parameters and to ensure repeatable quality. Suffice to say, the adjustment of manufacturing parameters can lead to the adjustment of micro strut and node deformation characteristic and micro lattice collapse behaviour, and hence the deformation and collapse of larger structures, e.g. blocks and sandwich panel cores. Note, that only a single laser spot occurs at the node, in order to minimise material volume.

20 mm^3 blocks were manufactured in the SLM250 machine [8]. The blocks were 'grown' from a steel bed plate. This means that blocks had to be cut from the bed plate using electrical discharge machining. Sacrificial pillars were included in the block lattice design, connecting the block to the bed plate.

Uniaxial block compression tests were conducted on 20 mm cubed lattice blocks placed between lubricated compression platens on an Instron 4024 universal test machine. This gives an unconstrained loading and it should be noted that BCC lattices are highly sensitive to block constraint [10]. A crosshead displacement rate of 0.5 mm/min was adopted in the elastic region and 1 mm/min in the plateau and densification regions of the load–displacement curves. The engineering stress was calculated from the applied load divided by the uncrushed cross sectional area and the engineering strain was taken to be the crush length divided by the uncrushed block height. It should be noted that these stress and strain measurements are not fundamental but provide a simple means of comparing different tests. It should also be noted that as the BCC block crushes it expands [8]. Also strain localisation may occur during crush, meaning that strain is not constant through the height of the block. Load was recorded from the load-cell and an extensometer was attached to the upper and lower compression platens recording the displacement at a rate of 10 samples per second.

Table 2
Parent material properties from micro strut tests.

Parent material W/μs	SS316L	TB[a][39]	Ti 6 4	TB[40]	Al 5056H38
	140/500		200/1000		
	SLM		SLM		Data sheet[41]
Property					
E (GPa)	140	205	45	115	71
E_{SLM}/E_{TB}	0.67		0.39		
E_{TB}/ρ_p (GPam^3 kg^{-1})	0.026		0.024		
$\sigma_{0.2}$ (MPa)	144	310	240	898	345
$\sigma_{0.2SLM}/\sigma_{0.2TB}$	0.46		0.27		
σ_{TB}/ρ_p (MPam^{3}kg^{-1})	0.039		0.192		
σ_{uts} (MPa)	280	620	280	996	415
$\sigma_{utsSLM}/\sigma_{utsTB}$	0.45		0.28		
ε_f	0.16	0.50	0.01	0.10	0.15
$\varepsilon_{fSLM}/\varepsilon_{fTB}$	0.32		0.10		
ρ_p (kgm^{-3})	7860	7860	4680	4680	2700
Average diameter (μm)	197 ± 17		372 ± 28		

SLM – as built, TB – Text book.
[a] Cold annealed.

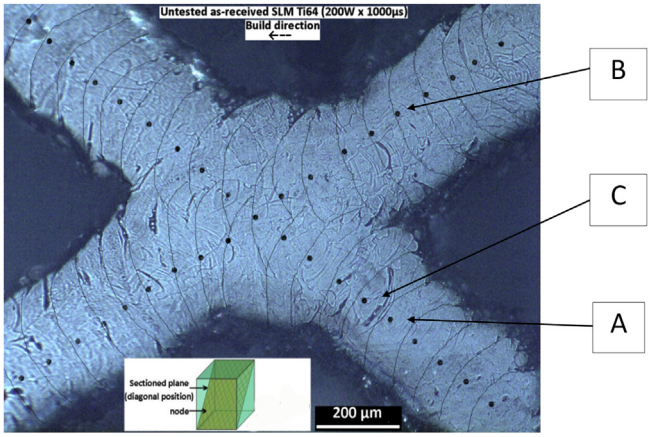

Fig. 5. Section detail in the vicinity of a node (Ti 6 4/200/1000). Build direction from right to left. A, B, C are laser focus points at increasing times. Estimated globule boundaries are outlined.

Four Ti 6 4 manufacturing routes are discussed in this paper, namely:

A. 180 W × 500 μs SLM
B. 180 W × 500 μs HIPed
C. 200 W × 1000 μs SLM
D. 200 W × 1000 μs HIPed

where the first term is the laser power in W, and the second term is laser exposure time in μs. SLM is as built, and HIPed is Hot Isostatic Processing.

Hot Isostatic Pressing (HIP) is a manufacturing process used to reduce the porosity of metals. This improves the mechanical properties, and workability. The HIP process subjects a component to both elevated temperature and isostatic gas pressure in a high-pressure containment vessel. The pressurising gas most widely used is argon and an inert gas is used, so that the material does not chemically react. Pressure is applied to the material from all directions (hence the term "isostatic") and the process is complex requiring specialist equipment [42]. In this case, the Ti 6Al 4V micro lattice blocks were treated at 930 °C under a constant pressure of 100 MPa for 2 h.

Fig. 6 shows that the collapse mode of the Ti 6 4 block (unconstrained block) is different to the stainless steel case [8,9]. The SS316L case was discussed in detail by Ushijima et al. [10], and they showed that block collapse was controlled by plastic hinges in the vicinity of the node. In the case of Ti 6 4, local rupture occurs at individual nodes, giving rise to shear bands in the block. The effect of HIPing is to increase ductility – less fragmentation can be seen in Fig. 6(b) for the HIP case.

Fig. 7 shows detailed micro strut failure in the Ti 6 4 block, showing that material rupture occurs near the nodes. This shows the importance of the strain to rupture parameter given in Table 2 and any increase in this will delay block total collapse. Detailed study of node deformation and rupture is required. This includes confidence in quality of manufacture, the detailed modelling of node geometry (taking into account actual quality), and the accurate use of mechanical properties from strut tensile tests, in the three-dimensional finite element modelling of deformation and rupture of the node.

Fig. 8(a)–(c) gives compression stress and strain data for three out of the four blocks under compression. Fig. 8(a) and (b) shows that the effect of HIPing is to improve ductility but to reduce initial crush stress. Fig. 8(b) and (c) shows that increasing laser power and exposure time leads to increase in initial crush stress, and maximum crush stress but a loss in ductility. Song et al. [43] discuss the effects of laser power and scanning speed on SLM Ti64 surface quality and mechanical properties. They attribute the effects to different

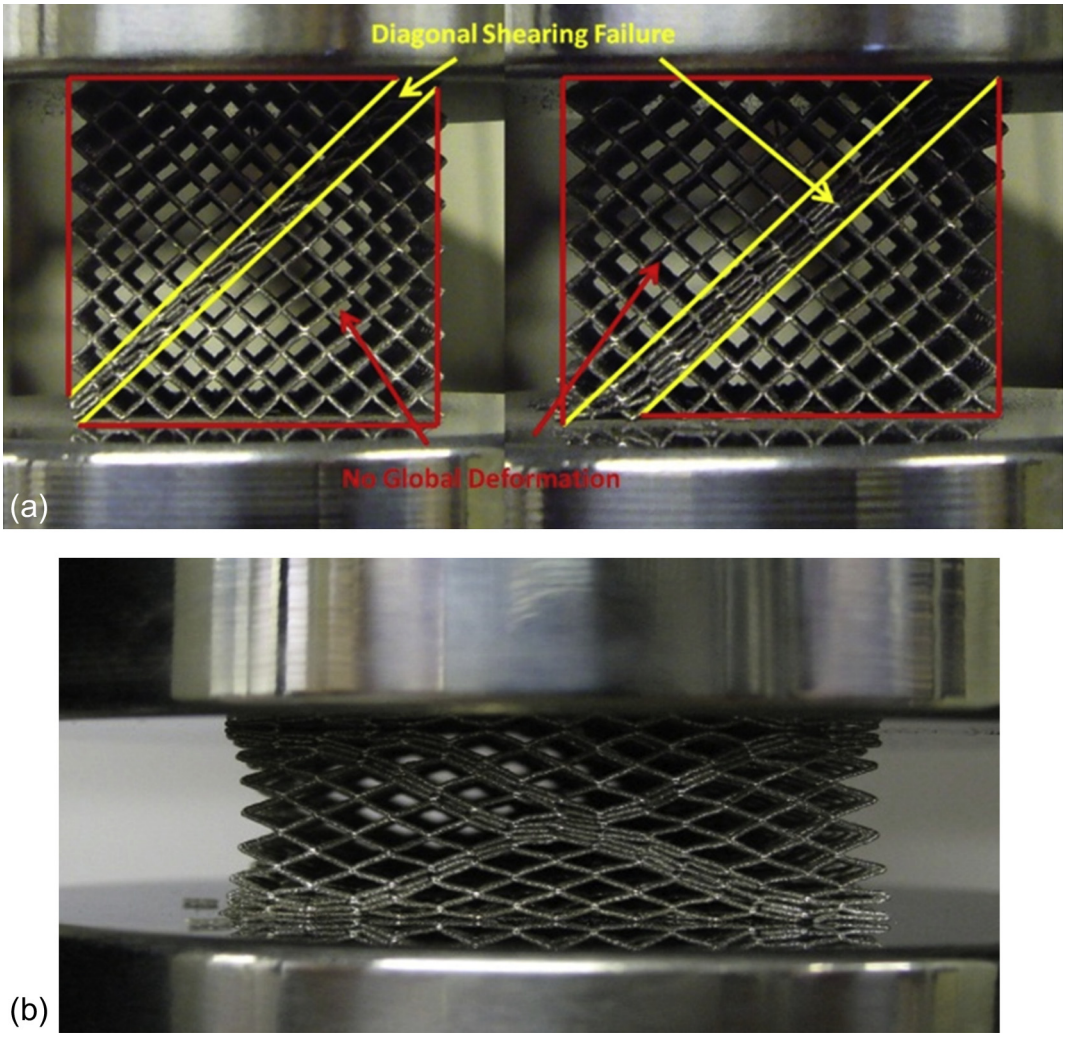

Fig. 6. The quasi-static crush behaviour of (a) 2 repeat tests for the SLM Ti64 lattice block and (b) HIPed Ti64 lattice block (Manufacturing parameters: Power = 180 W and Exposure Time = 500 μs).

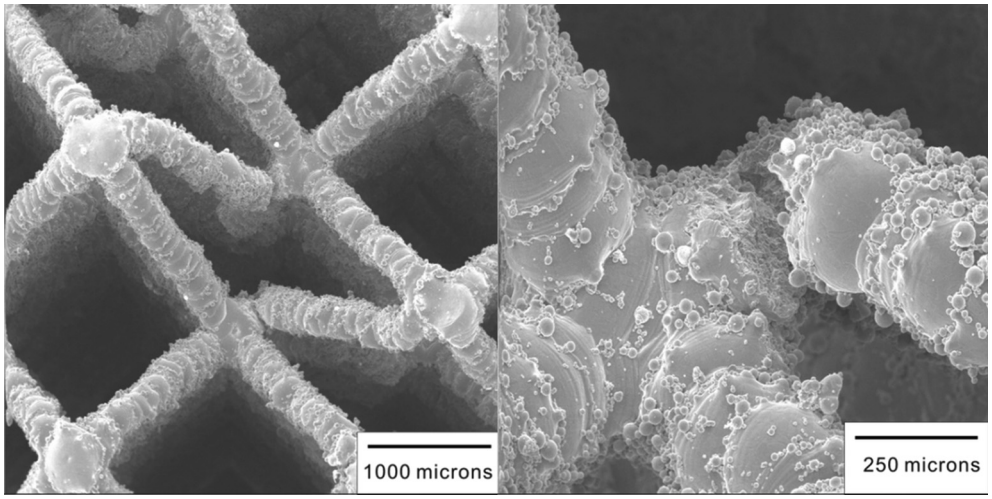

Fig. 7. Scanning electron microscope images of Ti 6 4 block detail at 2.2 mm crush, SLM, 180 W/500 μs.

melting mechanisms. It was decided, in this paper, to mainly focus on increasing yield stress and strength [200 W/1000 μs]. Also, given the complexity of the HIPing process, and variabilities due to other manufacturing process parameters, it was decided to test some panel specimens with the core, as built.

The diameter (d) of struts in a micro block can be calculated as follows [10]:

$$V = \sqrt{3}\pi N^3 d^2 L \tag{1}$$

where V = volume of material, N = number of cells = 8, d = strut diameter, L = cell length = 2.5 mm. The mass of the block, m_b, is given by:

$$m_b = V\rho_p \tag{2}$$

where ρ_p is the density of the parent material. Hence, the diameter (d) of the micro strut is given by:

$$d = \sqrt{\frac{m_b}{\rho_p \pi N^3 L\sqrt{3}}} = 0.0042\sqrt{m_b} \tag{3}$$

for steel, and:

$$d = 0.0055\sqrt{m_b} \tag{4}$$

for Ti 6 4. This means an average strut diameter can be estimated from measuring the mass of the block.

Table 3 summarises the block compression results. Due to lack of definition of initial crush stress, the stress at 2% strain is taken. The strut diameter increases with increasing laser power and exposure time. This is a result of increased melt pool diameter and this effect is discussed by Rehme [7]. E_B/ρ^* is markedly higher for the 200/1000 case – indicating stiffer nodes. σ_{2B}/ρ^* values are similar for all manufacturing routes, as is σ_{ultB}/ρ^*. This indicates a minimal effect of HIPing on initial crush and ultimate crush stresses. Block compression strain to failure increases due to HIPing but reduces with increased laser power and exposure time. In the panel tests (see below), cores with three Ti 6 4 manufacturing routes will be considered.

5. Experimental procedure for panels for SS316L and Ti 6 4

The woven carbon epoxy skin selected for this study was Gurit EP121-C15-53 [44]. This is a woven fabric of 3 k HTA carbon fibre, 193 gsm, plain weave, pre impregnated with 53% epoxy resin EP121. This is a highly toughened and self extinguishing resin system, with excellent adhesion to core materials and a short curing time. It is used for aircraft parts, e.g. passenger floor and secondary structures [44].

It was decided to compare sandwich panel performance for micro lattice cores, with those with aluminium honeycomb cores. The aluminium honeycomb selected was Hexcel CR111-1/4-5056-0.001N-2.3 [45]. The CR111 refers to corrosion resistance, ¼ refers to cell size in inches, 5056 refers to the alloy, 0.001 N refers to the foil thickness (non perforated) and 2.3 refers to the honeycomb density in lb/ft^3. The aluminium alloy is tempered to H39 state, however due to lack of data in the open literature, mechanical properties for H38 temper are given in this paper. This is a general purpose grade for aerospace core materials and has been studied extensively [46].

Stainless steel 316L and Ti64 micro lattice panels with cell size = 2.5 mm and with overall dimensions of 100 × 100 × 20 mm were manufactured using the SLM process. These were 'grown' from a steel bed plate in a manner similar to the blocks. The cores were 'grown' from one of the 20 mm by 100 mm sides and again sacrificial vertical pillars were included in the lattice adjacent to the bed plate [8]. Usually, 6 core blocks were manufactured at one time, and these were cut off the bed plate using electrical discharge machining.

The aluminium honeycomb cores were cut from 20 mm thick honeycomb material, and cut into the same dimension to the SLM panels. These core materials were then compression moulded with four plies plain weave carbon epoxy skins to form small panels. Fig. 9(a) shows the hot press used for producing the sandwich structures. The applied pressure was maintained below the yield stress of the core material, and was 0.5 MPa. The cure conditions are given Table 4. The resulting sandwich panels showed excellent bonding at the core–skin interface, see Fig. 9(b). This bond line has been studied in detail and the debonding strength has been shown to be very high [36].

The resulting sandwich panels were then placed on four hemispherical supports (10 mm diameter) and subjected to impact from a 10 mm diameter hemisphere attached to a drop weight machine, see Fig. 10. The impact machine was built 'in house', and had a

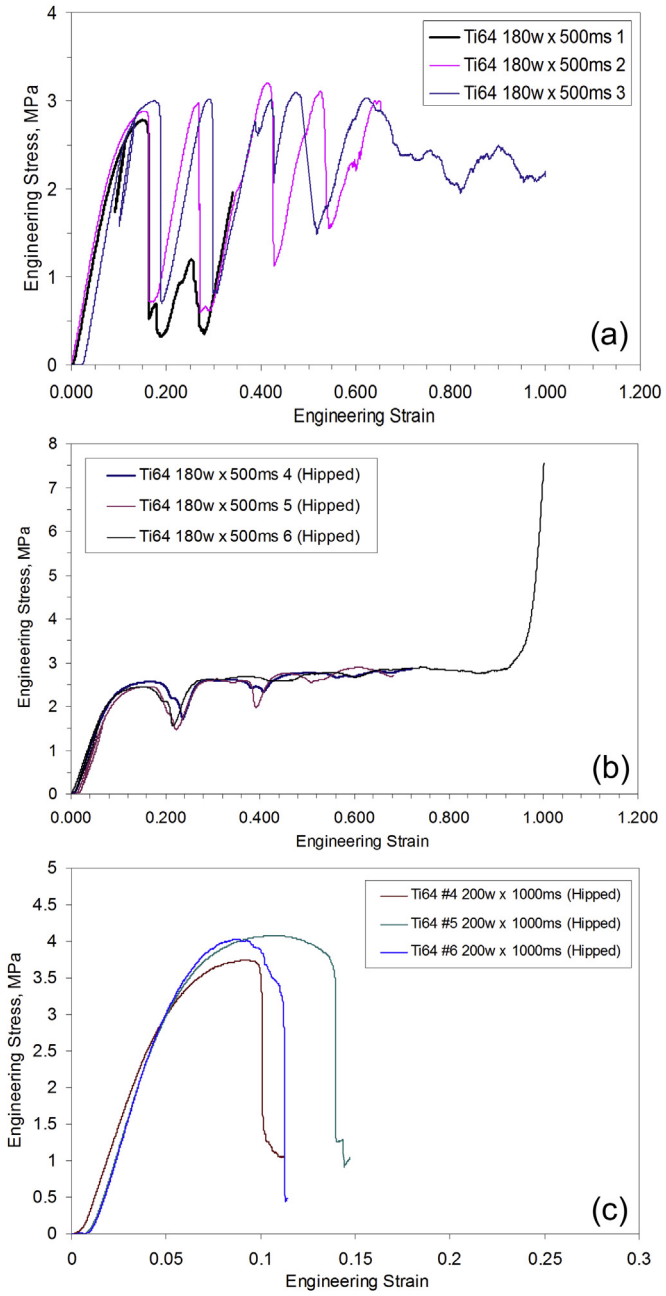

Fig. 8. Ti 6 4 block compression engineering stress vs. strain data: (a) As built (180 W/500 μs) and (b) HIPed at 180 W laser power and 500 μs laser exposure time and (c) HIPed laser power = 200 W and laser exposure time is 1000 μs (ms = microseconds).

height of 2 m with the impact mass being guided on steel rails [36]. The motivation for the four hemispherical supports was for ease of subsequent finite element simulation e.g. well defined boundary conditions [47]. The details of the sandwich panels and impact masses are given in Table 5.

Force versus displacement data was obtained using a Motion Pro 4 10,000 fps high-speed video camera [48]. Images were processed to give velocity versus time for the impactor using Pro Analyst Software [49]. The derived velocity curve was filtered using a digital Butterworth 700 Hz low pass filter. The filtering was required to suppress vibrations in the measuring system and the filter frequency was selected as a balance between filtering out unwanted noise without truncating the base signal [36]. Displacement, acceleration and force were derived from the velocity data. Post impact test damage was quantitatively assessed. Dent depth was measured using a clock gauge. Table 5 summarises the tests and Table 6 gives the drop heights for the small panels.

The average micro strut diameter (d) for these small BCC panels can be calculated in a similar manner to equations (1)–(4). In this case:

$$V = \sqrt{3}\pi N_1 N_2 N_3 d^2 L \tag{5}$$

where $N_1 = N_2 = 40$ and $N_3 = 8$, V is the volume of material, and L is the cell length. Hence:

$$V = 174.43 d^2 = \frac{m_p}{\rho_p} \tag{6}$$

where m_p is the mass of the panel block and ρ_p is the density of the parent material.

Therefore:

$$d = \sqrt{\frac{m_p}{174.4\rho_p}} = 0.000854\sqrt{m_p} \quad \text{for steel} \tag{7}$$

$$d = \sqrt{\frac{m_p}{174.4\rho_p}} = 0.001107\sqrt{m_p} \quad \text{for Ti 6 4} \tag{8}$$

So, again, an average diameter of micro strut can be derived from core mass. The diameter of the struts for the BCC core for Ti 6 4 (200 W/1000 μs) is 342 μm, whereas from the single strut, d = 372 μm. For SS316L these values are 226 μm and 197 μm, respectively. These differences are a result of the different mechanics of strut formation in the two cases as well as differences in the method of diameter assessment.

6. Sandwich panel results

Impact load versus displacement data of the stainless steel 316L sandwich panels are shown in Fig. 11. The initial non-linearity of the

Table 3
Mechanical properties from Ti64 block tests (A, B, C are the manufacturing parameters).

	Strut diam μm	E_B MPa	E_B/ρ^* MPam^3/kg	σ_{2B} MPa	σ_{2B}/ρ^* MPam^3/kg	σ_{ultB} MPa	σ_{ultB}/ρ^* MPam^3/kg	ε_{fB}	Mass 10^{-3} kg	ρ^* kgm^3
A/B/C										
SLM/180/500	263	11.43	40	2.0	7.0	2.8	10.0	0.160	2.28	285
SLM/180/500	263	11.43	40	2.0	7.0	2.9	10.0	0.160	2.28	285
SLM/180/500	263	11.43	40	2.0	7.0	3.0	10.0	0.195	2.28	285
HIP/180/500	263	25.0	88	2.0	7.0	2.4	8.0	0.210	2.28	285
HIP/180/500	263	25.0	88	2.0	7.0	2.4	8.0	0.210	2.28	285
HIP/180/500	263	25.0	88	2.0	7.0	2.5	8.0	0.240	2.28	285
HIP/200/1000	296	57.0	157	2.6	7.0	3.7	10.0	0.100	2.90	363
HIP/200/1000	296	57.0	157	2.7	7.0	4.0	10.0	0.115	2.90	363
HIP/200/1000	296	57.0	157	2.9	7.0	4.0	10.0	0.140	2.90	363

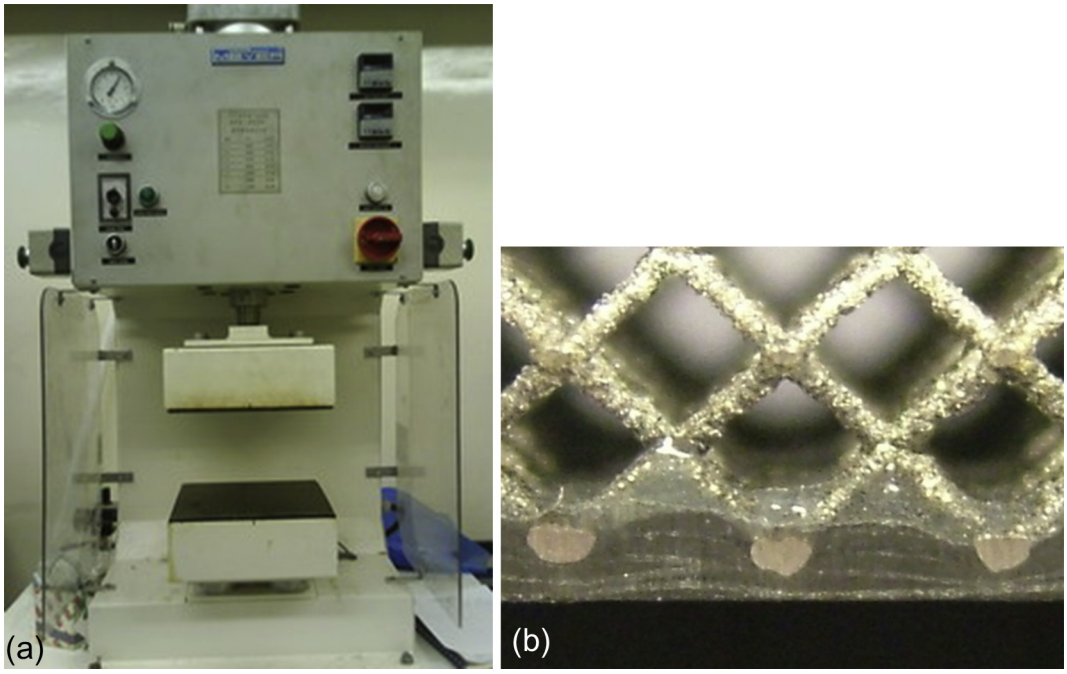

Fig. 9. (a) Hot press for manufacture of sandwich panels, and (b) skin-core bond details of SS316L lattice core and CFRP skins.

Table 4
Skin material parameters[44].

Prepreg material	Skin lay-up	Areal density g/m^2	Tensile modulus GPa	Tensile strength MPa	Cure temperature/time °C/min.
Plain weave Carbon fibre/epoxy matrix	4 ply 0/90° – nominal thickness 1.1 mm	410 ± 15	58 (8 ply)	850 (8 ply)	120/90

traces is due to upper skin damage and the reduction in the post maximum load is associated with the perforation process. It has been shown that impactor penetration for a given impact energy is similar between a fully supported and a four point supported panel [50]. However, greater levels of global bending were observed in the supported case. Fig. 11 shows a lack of rate sensitivity, although the tests are only over a restricted range of impact velocities.

Similar corner supported low velocity tests were carried out with the Ti64 #1–#7 BCC micro lattice sandwich panels and the honeycomb #1–#4 sandwich panels using an impact mass of 2.07 kg. Fig. 12(a) shows the load vs. displacement curves for Ti64 lattice core and Fig. 12(b) aluminium honeycomb core sandwich panels following the corner supported impact tests at different energies. Both figures have SS316L data. The large impactor displacements shown in Fig. 12 are a result of panel deformation and perforation. It can be seen from Fig. 12(a) that Ti64 lattice core manufactured using laser power and laser exposure time of 200 W and 1000 μs showed better impact resistance performance than that of manufactured at 180 W and 500 μs, although the latter offered better ductility.

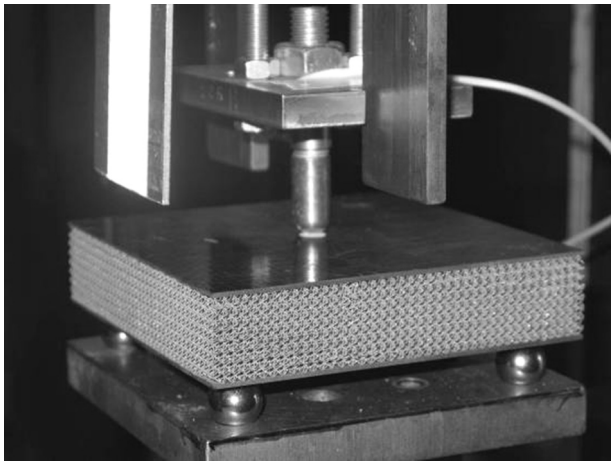

Fig. 10. Panel supported at four corners, with impactor. Panel size = 100 mm × 100 mm. Distance between supports = 76 mm.

In Fig. 12(a), Ti 6 4 #4–7 (200/1000) show higher perforation loads as compared with Ti 6 4 #1–3 (100/500). This is attributed to increased micro strut diameter in the former case, with a small improvement in properties (see Table 3). Ti 6 4 #4 is non-HIPed and shows the lack of ductility in the core during perforation. There is more rate dependence for the 200/1000 case (Ti 6 4 #4–7). After full perforation, Ti 6 4 (SLM/200/1000) offers the most resistance to the impactor. All Ti 6 4 load vs displacement traces are markedly above the SS316L trace. In Fig. 12(b), the honeycomb is less rate sensitive as compared with the Ti 6 4 micro lattice. Again, the SS316L curve has been shown for comparison.

Fig. 13(a) shows a top view and cross section for SS316L post impact of 8.8 J. A feature of the SS316L is the ductility causing struts to deform down into the damage zone. This means that strut damage spreads out from the perforation damage. This phenomenon has been discussed in detail in [50]. Fig. 13(b) shows photos for Ti 6 4 panel from a CT scan (Phoenix X-ray Nanotom (Wunstorf, Germany) High Resolution CT). The top view is taken at a depth of two cells (4 mm). It can be seen that damage is much more localised

Table 5
Summary of drop weight panel tests and panel properties.

Panel ID	Core type (cell size -mm)	Manufacture param (μs)	Drop mass (kg)	Panel mass (kg)	Panel thickness (mm)	Core mass (kg)	Micro strut diameter (μm)	Core density kg/m^3 (relative density)
316L #3–#6	BCC lattice (2.5)	500 (140)	0.88	0.070	21	0.037	226	185 (2.3%)
Ti64#1–#3	BCC lattice (2.5)	HIP 500 (180)	2.07	0.072	21	0.039	297	195 (4.4%)
Ti64 #4–#7	BCC lattice (2.5)	HIP 1000 (200)	2.07	0.096	22	0.062	342	310 (7.0%)
Honeycomb #1–#5	Aluminium honeycomb	–	2.07	0.042	21.5	0.008	–	38 (1.4%)
Ti64 #8–10	BCC, Z lattice (2.5)	1000 (200)	2.07	0.106	21	0.074	335	370 (8.3%)
Ti64 #11, 12	BCC lattice (2)	1000 (200)	2.07	0.130	22	0.092	310	460 (10.4%)

Table 6
Drop heights and panel IDs for panel tests (seeTable 5 for panel details).

	Panel ID	#1	#2	#3	#4	#5	#6	#7	#8	#9	#10	#11	#12
Drop height (mm)	316L	–	–	770	1140	970	1500	–	–	–	–	–	–
	Ti64	500	1000	1000	1000	250	500	750	1000	500	650	500	650
	Honeycomb	500	1000	250	370	450	–	–	–	–	–	–	–

due to the less ductile nature of the Ti 6 4. This has implications for post impact repairability [28]. Fig. 13(b) also shows the quality of image for this case, and shows the potential of the CT technique for study of not only nondestructive testing but also for 'as built' quality of manufacture. The latter is essential if these micro lattice materials are to be used in high performance load bearing structures. Fig. 13(b) also shows the quality and reproducibility of the micro lattice structure produced using SLM.

Fig. 13(c) shows damage for the honeycomb cored panel, showing more localised damage as compared to the SS316L case. Fig. 14 shows a comparison of the specific impact performance of sandwich panels based on four different core materials. The specific impact energy is the impact energy divided by the density of the panel, and the dent depth was measured by a clock gauge. Here, it is clear that the aluminium honeycomb core based sandwich panels show better specific performance than lattice core based sandwich panels. The performance of aluminium foam (Alporas, Shinko Wire Company, Amagasaki City, Japan) cored panels have been included for completeness. The same CFRP skins were used for all panels.

Shen et al. [9] have discussed the effect of changing micro structure geometry, e.g. BCC, Z or F2,BCC [7], and cell size, 1 mm–4 mm. Fairly obviously, as cell size reduces, the density, stiffness and strength increase. Also, adding extra struts over the BCC topology will increase the density of the lattice material. However, Ti 6 4 BCC, Z (2.5 mm) and BCC (2 mm) micro lattice configurations did not show a marked improvement in specific penetration performance (see Fig. 14).

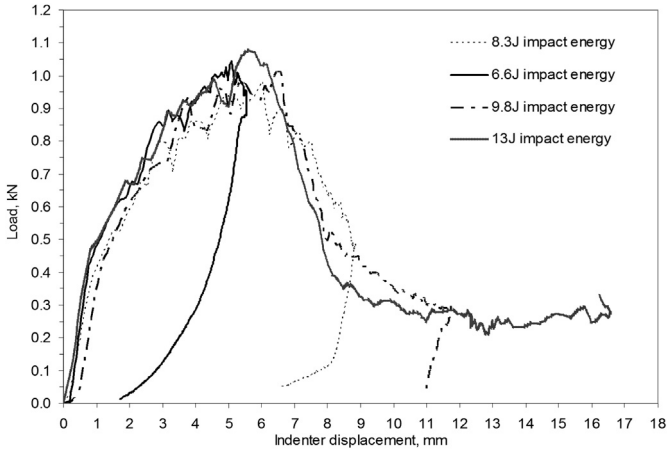

Fig. 11. Load vs impactor displacement for various impact energies for 316L stainless steel cored sandwich panel under four point support.

7. Discussion

The approach taken in this paper has been to discuss manufacturing process and material properties in parallel with structural performance. The three are intimately linked in the case of additive layer manufacture, and detailed structural analysis can only be achieved when the realised structure is fully defined and

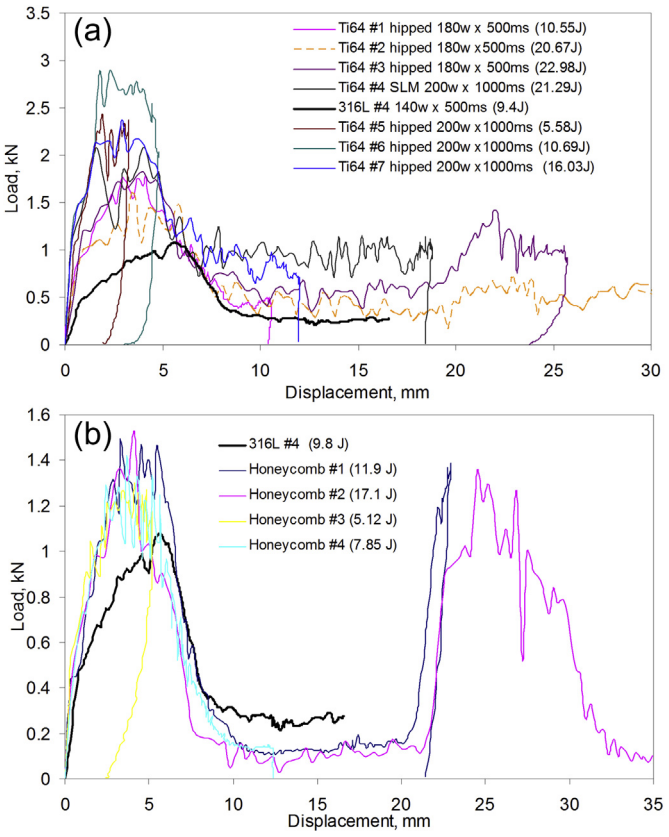

Fig. 12. Impactor load–displacement curves of sandwich panels based on (a) the Ti64 lattice core and (b) the aluminium honeycomb core for corner supported low velocity impact tests. Stainless steel 316L data shown for comparison. ms = microseconds. Impact energy in brackets.

quantified. The BCC 2.5 mm Ti 6 4 (HIPed/200 W/1000 μs) micro lattice show improved specific impact perforation performance over SS316L. This is attributed to the lower density of Ti 6 4 parent material. However, as shown in Table 2, mechanical properties of the present materials manufactured using SLM is non optimal.

In the case of SLM SS316L, $\sigma_{0.2SLM}/\sigma_{0.2TB} = 0.46$, $\sigma_{utsSLM}/\sigma_{utsTB} = 0.45$ and $\varepsilon_{fSLM}/\varepsilon_{fTB} = 0.32$ compared with text book values. SS316L cannot be hardened using heat treatment and it is proposed that these reduced tensile properties are a result of surface variabilities and imperfections. In the case of SLM Ti 6 4, $\sigma_{0.2SLM}/\sigma_{0.2TB} = 0.27$, $\sigma_{utsSLM}/\sigma_{utsTB} = 0.28$ and $\varepsilon_{fSLM}/\varepsilon_{fTB} = 0.10$ compared to text book values. Ti 6 4 is much more sensitive to thermal treatment. A complex technique of HIPing has been tried here, but from Fig. 8 it can be seen that there is a complex relation between HIPing and laser power/duration. It is proposed that HIPing is currently too complex in the context of current manufacturing status, and that a more conventional heat treatment is required [51].

Hence, there is most scope to improve the performance of Ti 6 4, given the relatively poor mechanical properties and surface quality from SLM, especially strain to failure (see Table 2). It would be useful to revisit the Ti 6 4 manufacturing process to ensure the minimising of any impurities, to optimise the laser power and exposure parameters, and to fully utilise post manufacture heat treatment. Not only will heat treatment improve microstructure and ductility, but also surface imperfections and residual stress [52] and hence variability in mechanical performance. Related to this is a need for detailed study of the deformation of the node, so as to adjust laser parameters and hence optimise the progressive collapse of BCC micro lattice structures. This should include a three-dimensional finite element analysis with full plasticity and rupture modelling. However, such issues as accuracy of FEA geometry, and appropriateness of plasticity and rupture models needs to be clarified.

Ushijima et al. [10] developed a block collapse analysis for the SS316L BCC micro lattice, assuming plastic collapse at nodes. They related block collapse stress (σ_{pl}) to micro lattice material properties and geometry:

$$\sigma_{pl} = \frac{\rho^*}{\rho_p}\frac{4\sqrt{6}}{9}\sigma_0\frac{d}{L} \tag{9}$$

Where ρ^* is the density of the lattice, ρ_p is the density of the parent material, σ_o is the flow stress of the parent material, d is the strut diameter and L is the cell length. Hence, for this mode of collapse (assuming no rupture), a doubling of flow stress will double the block collapse stress. Assuming a cylindrical volume of deformation for panel perforation, this would lead to a halving of the dent depth for a given impact energy. This would bring the Ti 6 4 micro lattice into direct competition with the honeycomb (see Fig. 14).

Only one structural performance aspect of micro lattice structures has been considered here, namely foreign object impact.

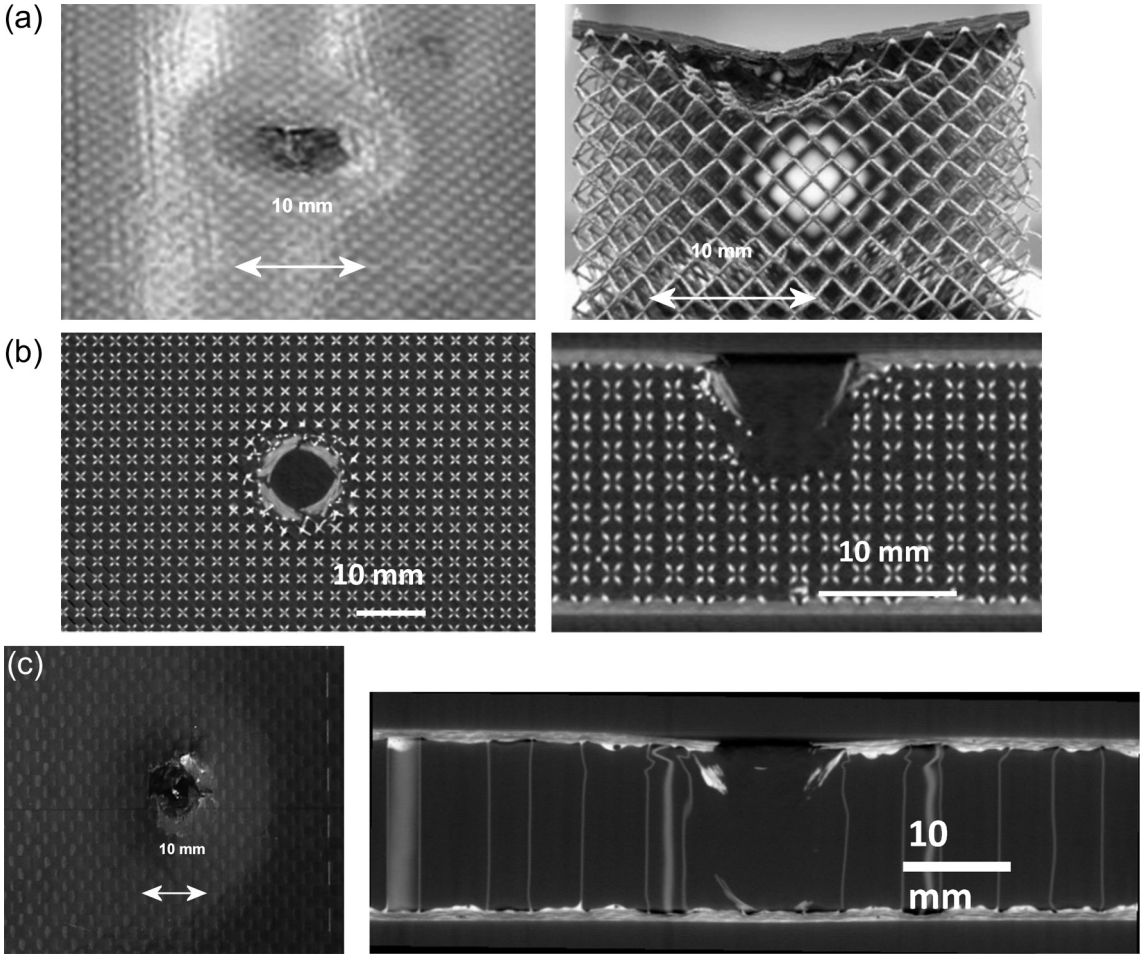

Fig. 13. Upper skin deformation and side section views of perforation for (a) the SS316L # 4 (8.8 J), (b) the Ti64 #3 (22.98 J) and (c) the honeycomb #1 (11.9 J) tests. Panels sectioned for (a) and (c), and CT scanned for (b).

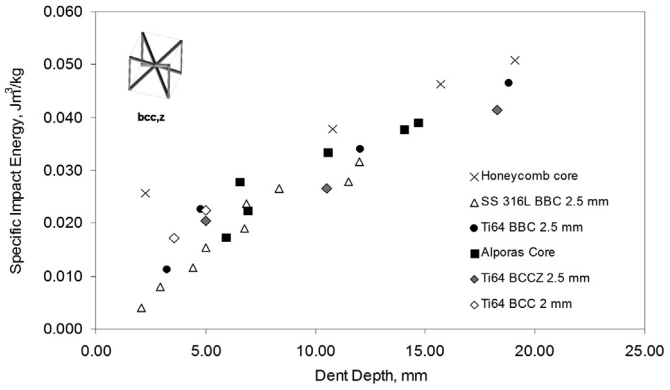

Fig. 14. Specific impact energy vs. dent depth of sandwich panels based on six types of core materials. Cell sizes shown for each lattice core type. Ti 6 4 BCC 2.5 mm #4–7 – HIPed/200/1000.

Major design variables in cores for sandwich construction are shear stiffness and strength. These shear properties for micro lattice structures have been discussed by Ptochos and Labeas [53] and Ushijima et al. [54]. They developed numerical models to predict the overall stiffness and strength of the cellular material in terms of micro strut orientation and length. Also, the fatigue behaviour of SLM components has been discussed by Santos et al. [55]. They identified the causes of low fatigue strength as porosity, impurities, and residual stresses. However, it should be noted that in this paper, due to the flexibility of the manufacturing process, the surface quality and topology of the micro lattice can be adjusted to mitigate fatigue occurrence and effect for a given structural application.

The SLM manufacturing process can realise graded and random structures, so allowing further optimisation of structural configuration for a given application [20]. Complex lattice structure have been defined in the literature, e.g. Kagome, Octet Truss etc. [7], but a major current limitation with the SLM process means that struts at angles below 25° to the horizontal cannot be built – due to the thermo mechanics of the formation of the micro strut. This means that complex lattice configurations may well have strut angles below this, even if the orientation of the build direction is optimised in three dimensions.

It should be noted that the blocks and cores take about 6 h to build given that such components contain over 1000 layers, but as previously stated, a number of components can be made at one time. A 250 mm^3 build envelope SLM machine was used here [8] but a 500 mm^3 build envelope SLM machine is currently being developed. In the latter machine, the laser system and scanning hardware and software are being improved, to speed up the SLM process and to reduce energy consumed and waste produced during manufacture.

8. Conclusions

The current Ti 6 4 BCC micro lattice structures have been shown to be able to compete with aluminium honeycomb from the point of view of Foreign Object Impact performance in aerospace sandwich panels. This performance should be significantly improved by fully exploiting the potential quality of the Ti 6 4 parent material. The SS316L BCC micro lattice structures have better quality and are less sensitive to build conditions. However, they have lower specific strength and so are less suited to high performance applications.

Panel foreign object impact performance could be further enhanced by quantifying micro inertia and material strain rate effects in the core and by adapting micro lattice structure architecture to improve impact performance. For the SS316L BCC case studied here, progressive collapse is dominated by plastic hinges in the vicinity of the node and so impact effects will relate to beam bending dynamics and rate dependence of the yield stress of the parent material. For the Ti 6 4 BCC case, material rupture becomes an issue and the rate dependence of this parameter will control impact progressive collapse performance.

The paper has addressed the application of a novel manufacturing technology to a widely used structural application, viz. open cellular cores. If the manufacturing technology is to be fully utilised, two major issues need to be addressed further. The most immediate major issue is to fully define, in detail, the quality of the micro lattice structure. This includes dimensional accuracy, surface quality, residual stresses, material microstructure, trace impurities, and hence variabilities in material and structural performance. The longer-term major issue is to rigorously define the relation between process – material – structural performance. An empirical parametric approach for manufacture has been taken here and reasonable quality structures have been obtained. However, if full quality and repeatable structures are to be realised, then a complete account of the material route from powder to final structure is required.

Finally, it should again be noted that the manufacturing process is continually being developed [17], and that further work is needed to make the process more competitive, from the points of view of speed and energy consumption, for use in high performance structural components [16–18].

Acknowledgements

This research was funded by EU FP6 Celpact and EPSRC grants EP/009398/1 and EP/C009525/1. Professor Xinhua Wu, Birmingham University, provided the HIPing. Dr Alastair Johnson, DLR, Stuttgart provided the CT scans. SLM equipment was developed by Dr Chris Sutcliffe, with funds from Stryker Orthopaedics. Mr Dan Hibbert helped on the figures. Ms Rafidah Hasan was supported by the Malaysian Government.

References

[1] Hermann AS, Zahlen PC, Zuardy I. Sandwich structures technology in commercial aviation. In: 7th International Conference on sandwich structures (ICSS-7), Aalborg 2005. p. 13–26.
[2] Heimbs S, Cichosz J, Klaus M, Kilchert S, Johnson AF. Sandwich structures with textile reinforced composite foldcores under impact loads. Comp Struct 2010;92:1484–97.
[3] Sypeck DJ. Cellular truss core sandwich structures. Appl Comp Mat 2005;12:229–46.
[4] Fleck NA, Deshpande VS, Ashby MF. Micro-architectured materials: past, present and future. Proc Roy Soc A 2010;466:2495–516.
[5] Queheillalt DT, Wadley HNG. Titanium alloy lattice truss structures. Mat Des 2009;30:1966–75.
[6] Yadroitsev I. Selective laser melting. Saarbrucken, Germany: Lambert Academic Publishing; 2009.
[7] Rehme O. Cellular design for laser freeform fabrication. Gottingen, Germany: Cuivillier Verlag; 2010.
[8] Tsopanos S, Mines RAW, McKown S, Shen Y, Cantwell WJ, Brookes W, et al. The influence of processing parameters on the mechanical properties of selective laser melted stainless steel micro lattice structures. J Manu Sc Eng 2010;132. 041011 p1–12.
[9] Shen Y, McKown S, Tsopanos S, Sutcliffe CJ, Mines RAW, W.J. The mechanical properties of sandwich structures based on metal lattice architectures. J Sand Struct Mat 2010;12:159–80.
[10] Ushijima K, Cantwell WJ, Mines RAW, Tsopanos S, Smith M. An investigation into the compression properties of stainless steel micro lattice structures. J Sand Struct Mat 2010;13(3):303–29.
[11] Labeas GN, Sunaric MM. Investigation on the static response and failure process of metallic open lattice cellular structures. Strain 2008;46:195–204.
[12] Jacobsen AJ, Barvosa-Carter W, Nutt S. Compression behaviour of micro scale truss structures formed from self propagating polymer wave guides. Acta Materialia 2007;55:6724–33.
[13] Schaedler TA, Jacobsen AJ, Torrents A, Sorensen AE, Lian J, Greer JR, et al. Ultralight metallic micro lattices. Science 2011;334:962–5.

[14] Parthasarathy J, Starly B, Raman S, Christensen A. Mechanical evaluation of porous titanium (Ti6Al4V) structures with electron beam melting (EBM). J Mech Beh Biomed Mat 2010;3:249–59.
[15] Cansizoglu O, Harrysson O, Cormier D, West H, Mahale T. Properties of Ti 6Al 4V non stochastic lattice structures fabricated via electron beam melting. Mat Sc Engg 2008;A482:468–74.
[16] Gibson I, Rosen DW, Stucker B. Additive manufacturing technologies. New York, USA: Springer; 2010.
[17] Kellens K, Yasa E, Renaldi R, Dewulf W, Kruth JP, Duflou JR. Energy and resource efficiency of SLS/SLM processes. In: International Solid Freeform Symposium No. 22, Austin, Texas 8–10 August 2011. p. 1–16.
[18] Warwick G. Adding value: additive manufacturing could bring much needed affordability to aerospace products. Aviation Week Space Technol November 1/8 2010:80–3.
[19] Mines RAW, Worrall CM, Gibson AG. Low velocity perforation behaviour of polymer composite sandwich panels. Int J Imp Engg 1998;21(10):855–79.
[20] Mines RAW. On the characterisation of foam and micro lattice materials in sandwich construction. Strain 2008;44:71–83.
[21] Smith M, Cantwell WJ, Guan Z, Tsopanos S, Theobald MD, Nurick GN, et al. The quasi static and blast response of steel lattice structures. J Sand Struct Mat 2010;13(4):479–501.
[22] Lee S, Barthelat F, Hutchinson JW, Espinosa HD. Dynamic failure of metallic pyramidal truss core materials – experiment and modelling. Int J Plast 2006;22:2118–45.
[23] Lee S, Barthelat F, Moldovan N, Espinosa HD, Wadley HNG. Deformation rate effects on failure modes of open cell Al. foams and textile materials. Int J Sol Struct 2006;43:53–73.
[24] Evans AG, He MY, Deshpande VS, Hutchinson JW, Jacobsen AJ, Carter WB. Concepts for enhanced energy absorption using hollow micro lattices. Int J Imp Engg 2010;37:947–59.
[25] Fang DN, Li YL, Zhao H. On the behaviour characterisation of metallic cellular materials under impact loading. Acta Mech Sin 2010;26:837–46.
[26] Mahmoudabadi MZ, Sadighi M. A theoretical and experimental study on metal hexagonal honeycomb crushing under quasi static and low velocity impact loading. Mat Sc Engg 2011;A528:4958–66.
[27] Polmear I. Light alloys. 4th ed. Amsterdam: Butterworth Heinemann; 2006.
[28] Morteau E, Fualdes C. Composites@Airbus damage tolerance methodology, ESAC-Ref X029 PR0608046. Chicago, IL, USA: Nat. Inst. For Aviat. Res; 2006.
[29] Stamp R. Manipulator V4.7.1 user manual. University of Liverpool; 2008.
[30] MCP Realizer II, SLM operating manual. MCP –HEK Tooling GmbH; 2006.
[31] Mullen L, Stamp RC, Brooks WK, Jones E, Sutcliffe CJ. Selective Laser Melting: a regular unit cell approach for the manufacture of porous titanium bone in growth constructs, suitable for orthopaedic applications. J Biomed Mat Res Part B Appl Biomat 2008:325–34.
[32] Deshpande VS, Ashby MF, Fleck NA. Foam topology: bending versus stretching architecture. Acta Mat 2001;49:1035–45.
[33] Deshpande VS, Fleck NA. Collapse of truss core sandwich beams in 3 point bending. Int J Sol Struct 2001;38:6275–305.
[34] Mines RAW, Girard Y, Fascio V. On the development of conventional and micro lattice metals as core materials in aerospace sandwich construction. In: Sampe Europe Conference and Exhibition, Paris, France 2009. p. 248–55.
[35] Techik TLS. Data sheet: Ti6Al4V powder, -45μm, particle spherical. Bitterfield, Germany: TLS Technik GmbH; 2008.
[36] Shen Y. High performance sandwich structures based on novel metal cores. University of Liverpool; 2009. (PhD thesis).
[37] Hasan R, Mines RAW, Fox P. Characterisation of selectively meltedTi 6Al 4V micro lattice struts. Procedia Eng 2011;10:536–41.
[38] Hasan R, Mines RAW, Tsopanos S. Determination of elastic modulus value for selectively laser melted titanium alloy micro strut. J Mech Engg Techn 2010;2(2):17–25.
[39] Cambridge Engineering Selector. Properties: titanium alpha beta alloy Ti-6Al-4V cast. [accessed 2012].
[40] Cambridge Engineering Selector. Properties: stainless steel austenitic AISI 316L wrought, cold annealed. [accessed 2012].
[41] Matweb Property Data, Data Sheet: aluminium 5056 H38 temper. [accessed 2012].
[42] Wu X. Review of alloy and process development of Ti Al alloys. Intermetallics 2006;14:1114–22.
[43] Song B, Dong S, Zhang B, Liao H, Coddet C. Effects of processing parameters on microstructure and mechanical property of selectively laser melted Ti-6Al-4V. Mater Des 2012;35:120–5.
[44] Gurit GmbH. Data sheet: EP121-C15-53. Kassell, Switzerland: Gurit GmbH; 2008.
[45] Hexcel Inc.. Data sheet: CTIII-1/4 -5056-0.001N-2.3. Stamford, CT, USA: Hexcel Inc.; 2012.
[46] Elnasri I, Pattofatto S, Zhao H, Tsitsiris H, Hild F, Girard Y. Shock enhancement of cellular structures under impact loading: Part I: Experiments. J Mech Phy Sol 2007;55:2652–71.
[47] Mines RAW, Tsopanos S, McKown ST. Verification of a finite element simulation of the progressive collapse of micro lattice structures. Appl Mech Mat 2011;70:111–6.
[48] Redlake Inc.. Operation manual: Motion Pro X4 high speed camera. Tallahasse, FL, USA: Redlake Inc; 2006.
[49] Xcitex Inc.. Operation manual: Pro Analyst Software, Version: Professional/ Workstation. Cambridge, MA, USA: Xcitex Inc.; 2006.
[50] Mines RAW, McKown ST, Tsopanos S, Shen Y, Cantwell WJ, Brooks W, et al. Local effects during indentation of fully supported sandwich panels with micro lattice cores. Appl Mech Mat 2008;13-14:85–90.
[51] Gilbert R, Shannon CR. Solution treating and ageing in heat treating of titanium and titanium alloys. In Asm Handbook, vol. 4. USA: ASM International; 1991.
[52] Casavola C, Campanelli SL, Papalettere C. Preliminary investigation on distribution of residual stress generated by the selective laser melting process. J Strain Anal 2009;44:93–104.
[53] Ptochos E, Labeas G. Shear modulus determination of cuboid metallic open lattice cellular structures by analytical, numerical and homogenisation methods. Strain 2012;48:415–29.
[54] Ushijima K, Cantwell WJ, Chen DH. Shear response of three dimensional micro lattice structures. Key Engg Mat 2011;452–453:713–6.
[55] Santos EC, Osakada K, Shiomi M, Kitamura Y, Abe F. Micro structure and mechanical properties of pure titanium models fabricated by selective laser melting. J Mech Engg Sc 2004;218:711–9.